

Using direct and indirect measurements of leaf area index to characterize the shrub canopy in an ombrotrophic peatland

O. Sonnentag^{a,*}, J. Talbot^{b,1}, J.M. Chen^{a,2}, N.T. Roulet^{b,1}

^a University of Toronto, Department of Geography and Planning, St. George Campus, Sidney Smith Hall,
100 St. George St., Room 5047, Toronto, Ont. M5S 3G3, Canada

^b McGill University, Department of Geography, Burnside Hall, 805 Sherbrooke West, Room 705, Montreal, Que. H3A 2K6, Canada

Received 29 August 2006; received in revised form 10 January 2007; accepted 2 March 2007

Abstract

Leaf area index (LAI) is an important ecological parameter that characterizes the interface between a vegetation canopy and the atmosphere. Indirect measurements of LAI using optical techniques such as the LAI-2000 plant canopy analyzer have been routinely conducted for different vegetation canopies including forests and agricultural crops. However, little attention has been paid to shrub canopies of peatlands, where microtopography presents an additional challenge in the optical measurement of shrub LAI. Based on an established equation for boreal forest canopies to derive LAI from “effective” LAI obtained from the LAI-2000 instrument, we evaluated the overall performance of this indirect measurement technique by comparing it with destructive sampling results for the shrub canopy of a precipitation-fed (ombrotrophic) peatland near Ottawa, Ontario, Canada. Under the assumption of no foliage clumping in the shrub canopy, we demonstrate that the contribution of woody canopy elements to light interception has to be taken into account. For this purpose, we determined species-specific woody-to-total area ratios for the five major shrub species. Furthermore, we evaluated the combined effect of microtopographic position of the measurement location and multiple light scattering within the shrub canopy on the measurements. Taking both the contribution of woody canopy elements to light interception and the combined effect of microtopography and multiple light scattering into account, the agreement between direct and indirect measurements of shrub LAI is good ($R^2 = 0.74$), and intercept and slope of the linear correlation are not significantly different from 0 ($p = 0.3575$) and 1 ($p = 0.7489$), respectively. The indirect approach refined through this study provides a reliable method for quick measurements of shrub LAI in ombrotrophic peatlands.

© 2007 Elsevier B.V. All rights reserved.

Keywords: Leaf area index; Shrubs; Peatlands; Direct measurement; LAI-2000; Microtopography; Multiple light scattering

1. Introduction

Peatlands are wetlands that accumulate partially decayed plant matter in the form of peat, with bogs and

fens as the most common types (Wheeler and Proctor, 2000). Bogs are precipitation-fed (ombrotrophic) and generally lack any other hydrological inputs, resulting in acidic and nutrient-poor conditions. Fens receive, in addition to precipitation, hydrological inputs from their surrounding mineral uplands in the form of surface and subsurface flow (minerotrophic). As a result, fens, commonly subdivided into poor and rich fens, are less acidic and nutrient-rich peatlands. While peatlands cover only 3% of the terrestrial land surface (Maltby and Immirzi, 1993), they are an extensive component of

* Corresponding author. Tel.: +1 416 946 7715;
fax: +1 416 946 3886.

E-mail address: oliver.sonnentag@utoronto.ca (O. Sonnentag).

¹ Tel.: +1 514 398 4111; fax: +1 514 398 7437.

² Tel.: +1 416 946 7715; fax: +1 416 946 3886.

the boreal and subarctic ecozones. For example, in Canada they cover about 14% of the terrestrial area (Tarnocai et al., 2000).

A number of field carbon flux measurements, paleoecological records, and model simulations have demonstrated that peatlands are an active component of the global carbon cycle (e.g., Lafleur et al., 2001; Clymo, 1998; Frohking et al., 2002; Roulet et al., 2006). The functional importance of peatlands in the global carbon cycle is rooted in their capability to act as long-term stores of carbon as peat. The accumulation of peat is the result of net primary productivity (NPP), the net gain of carbon through photosynthesis, persistently exceeding the decomposition of organic matter. With an average long-term apparent carbon accumulation rate of $15\text{--}30\text{ g C m}^{-2}\text{ yr}^{-1}$, peatlands have been acting as small but persistent carbon sinks since the beginning of their development after the last deglaciation (Turunen et al., 2002). As a result, peatlands store up to 450 Gt C or one-third of the global soil carbon (Gorham, 1991; Turunen et al., 2002).

Quantification of possible responses of peatland carbon dynamics to likely climatic changes as predicted by several General Circulation Models (GCM) still remains a big challenge because of the complexity of the interrelated physical, ecological, and biogeochemical feedbacks involved (Moore et al., 1998). Process-oriented ecosystem models of varying complexity such as the Boreal Ecosystem Productivity Simulator (BEPS, Liu et al., 1997) and the Peatland Carbon Simulator (PCARS, Frohking et al., 2002) are considered as promising tools to quantify the responses of peatland carbon cycle dynamics to likely climatic changes.

An important parameter of most process-oriented ecosystems models is the leaf area index (LAI). Some models use LAI as an input parameter (e.g., BEPS), while others generate LAI as a function of foliar biomass (e.g., PCARS). LAI is a dimensionless value of the amount of foliage area of a vegetation canopy and is defined as one-half the total radiation intercepting leaf area (all-sided) per unit ground horizontal surface area (Chen and Black, 1992). LAI characterizes the canopy–atmosphere interface of an ecosystem, and is thus related to precipitation interception, canopy microclimate, radiation extinction, and water, carbon, and energy exchange with the atmosphere, and also plays a role in the interception of atmospheric nutrient deposition. In the field, LAI can be determined with direct and indirect measurements (Bréda, 2003; Jonckheere et al., 2004).

Direct measurements of LAI are considered to be the most accurate and hence, play an important role in

validating indirect measurements (e.g., Chen et al., 1997; Küßner and Mosandl, 2000). All direct measurements have the disadvantage of being very time-consuming; they are two-step processes consisting of leaf collection by either harvesting (e.g., destructive sampling) or non-harvesting (e.g., litter traps) methods, and subsequent leaf area calculation based on either planimetric (e.g., scanning planimeter LI-3000, LICOR, Lincoln, NE, USA) or gravimetric (e.g., predetermined green leaf area-to-dry weight-ratios) methods (Jonckheere et al., 2004).

Indirect measurements of LAI are based on the inference of leaf area from another, more easily and faster measurable variable and are further subdivided into contact (e.g., inclined point method for low canopies or allometric techniques for forests) and non-contact (e.g., optical techniques based on light transmission through vegetation canopies using radiative transfer theory) methods (Bréda, 2003; Jonckheere et al., 2004). A practical, effective, and hence widely applied optical technique to determine LAI that has been successfully applied widely is the LAI-2000 (LICOR, Lincoln, NE, USA) plant canopy analyzer (Norman and Welles, 1991).

The LAI-2000 instrument measures canopy gap fraction at five zenith angles. The LAI estimate obtained from the LAI-2000 instrument is an “effective” LAI (LAI_e) calculated from the light interception of all canopy elements using a radiative transfer model, assuming a random spatial distribution of all light intercepting elements of the canopy (Chen et al., 1997). To derive the LAI of a vegetation canopy from LAI_e , Chen (1996) and Chen et al. (1997) demonstrate for boreal forest canopies that LAI_e has to be corrected for the contribution of woody canopy elements to light interception and for foliage clumping (i.e. their non-random spatial distribution) at three different spatial scales (branches, whirls and tree crowns, and groups of trees) for deciduous species and at four different spatial scales (shoots, branches, whirls and tree crowns, and groups of trees) for coniferous species. Several studies have demonstrated that the LAI-2000 instrument tends to underestimate LAI_e due to multiple light scattering, especially when the measurement was taken under non-ideal light conditions (Chen, 1996; Chen et al., 1997, 2006; Leblanc and Chen, 2001). Thus, a further correction of LAI_e should be applied to account for the effect of multiple light scattering within a canopy.

The multi-layer canopy of ombrotrophic peatlands is often characterized by the abundance of evergreen, and occasional deciduous shrubs and patches of open tree canopies, underlain by a continuous surface cover of

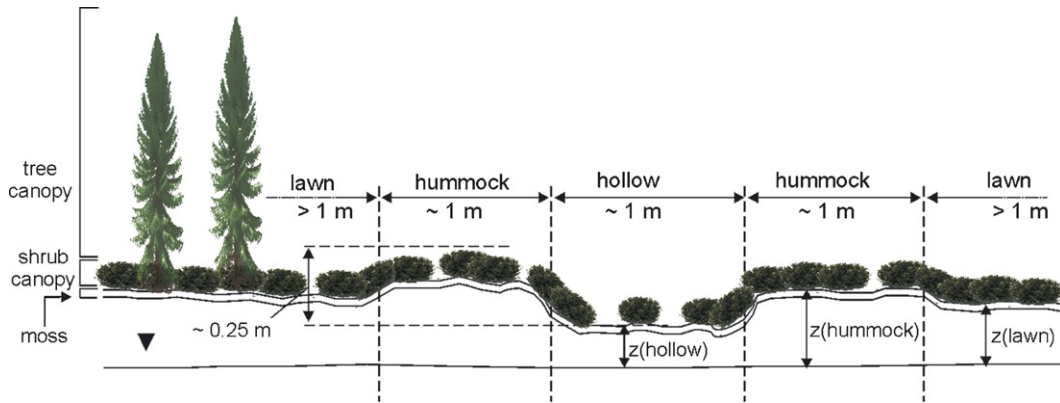


Fig. 1. Multi-layer canopy and relationship between microtopography and water table height of ombrotrophic peatlands (not drawn to scale).

different moss species (Fig. 1). A great part of the spatial variation of the overall species composition in peatlands can be explained by different heights (z) of the peatland surface above the water table due to microtopography (Bubier et al., 2006), resulting in a slightly undulating ground surface. Peatlands' microtopography comprises microforms including individual "wetter" depressions (hollows) and "drier" mounds (hummocks) of limited spatial extent ($\sim 1 \text{ m}^2$), and intermediate lawns covering larger areas ($> 1 \text{ m}^2$), with $z(\text{hummock}) > z(\text{lawn}) > z(\text{hollow})$ (Fig. 1).

Despite the importance of the shrub canopy in the overall hydrological and ecological functioning of peatlands (e.g., Lafleur et al., 2005; Moore et al., 2002), detailed studies focusing on peatland shrub LAI and its rapid, reliable quantification with a standard technique such as the LAI-2000 instrument are lacking. Our goal is to characterize the shrub canopy LAI as influenced by microtopography during the peak growing season of Mer Bleue bog near Ottawa, Ontario, Canada, whose shrub canopy composition is typical of ombrotrophic peatlands (Payette and Rochefort, 2001). We develop a quick and reliable method to determine shrub LAI in ombrotrophic peatlands. This method has been used to collect a large number of LAI data for developing remote sensing algorithms for separate tree and shrub LAI mapping in ombrotrophic peatlands (Sonnentag et al., in press). Our objectives are (i) to evaluate the overall performance of the LAI-2000 instrument based on the established equation of Chen (1996) and Chen et al. (1997) by determining the linear correlation between "true" shrub LAI obtained through destructive sampling and optically measured shrub LAI, and (ii) to investigate the combined effect of the microtopographic position of the LAI-2000 measurement location and multiple light scattering on optically measured LAI.

2. Materials and methods

2.1. Site description and plots

The Mer Bleue bog (45.4°N, 75.5°W) is a raised, ombrotrophic peatland, located in the Ottawa Valley-St. Lawrence Lowland physiographic region, about 10 km southeast of Ottawa, Ontario, Canada. The climate of the region is classified as cool continental. The bog covers a total area of about 28 km² and is roughly oval shaped with an east-west orientation. The western part of the bog is dissected by two east-west oriented longitudinal lobes of coarse-grained fluvial deposits, creating three separate arms (Lafleur et al., 2005). Peat accumulation began about 8500 years ago, with today's peat depths varying between about 2 and 5 m (Roulet et al., 2006). The gently domed central part of the Mer Bleue bog has an average elevation of approximately 69 m above sea level, resulting in an overall convex structure. Due to its geomorphology, surface and sub-surface water is shed from the central part of the bog towards its margin, where it drains away. As a result of the acidic and nutrient-poor conditions, the vegetation structure of the Mer Bleue bog is characterized by dominant evergreen shrubs (*Chamaedaphne calyculata*, *Ledum groenlandicum*, *Kalmia angustifolia*, *Kalmia polifolia*, *Andromeda glaucophylla*), deciduous shrubs (*Vaccinium myrtilloides*), and sparse patches of sedges (*Eriophorum vaginatum*) and black spruce (*Picea mariana*) and tamarack (*Larix laricina*) trees, and occasional grey birch (*Betula populifolia*) trees. Characteristic features of the Mer Bleue bog are distinct microforms consisting of hollows, hummocks, and lawns, with a mean relief between hollows and hummocks of 0.25 m (Lafleur et al., 2005). The surface cover is composed of different species of *Sphagnum*

Table 1
Summary of species composition, percent cover, and mean shrub height of the 33 plots considered in this study

Microform	#	Mean cover [%] (standard deviation, %)				Mean shrub height [cm] (standard deviation, cm)
		Evergreen shrubs	Deciduous shrubs	Sedges	Total	
Hollow	9	30.0 (16.4)	1.7 (3.5)	8.9 (16.4)	40.6 (18.8)	15.3 (3.4)
Evergreen hummock	9	86.7 (6.1)	2.8 (2.6)	1.1 (2.2)	90.6 (8.1)	19.3 (3.8)
Deciduous hummock	6	27.5 (12.9)	51.7 (13.7)	1.7 (4.1)	88.8 (16.6)	29.7 (8.4)
Lawn	9	60.6 (14.9)	2.8 (6.7)	2.8 (2.6)	66.1 (15.2)	14.8 (2.6)

moss (*Sphagnum angustifolium*, *Sphagnum capillifolium*, *Sphagnum magellanicum*, and *Sphagnum fuscum*).

We measured shrub LAI directly and indirectly in 33 plots of 0.5 m × 0.5 m at different microtopographic locations on the western, upslope side of a drainage ditch that dissects the eastern part of the bog. We distinguish, based on the dominant shrub type, among evergreen hollows, evergreen hummocks, deciduous hummocks, and evergreen lawns. The plots were delimited and inventoried at the beginning of summer 2005 and randomly located but evenly distributed for each microform at a distance of 30, 60, and 200 m away from the drainage ditch along a perpendicular transect. At a distance of 200 m from the drainage ditch, no deciduous hummock was present so only hollows, evergreen hummocks, and lawns were represented, resulting in 33 plots in total. Species composition, percent cover, and mean height of each species were estimated prior to clipping (summarized in Table 1). Trees were absent in all 33 plots.

The area containing the plots is influenced by the drainage ditch and is generally characterized by increasing water table depths with decreasing distance to the ditch. Peatland plant biomass increases with increasing water table depth (Bubier et al., 2006). Since the plots were located along a water table gradient, a greater range of shrub LAI values could be sampled.

2.2. Direct LAI measurements

Shrub LAI of all 33 plots was measured directly and indirectly in August 2005. The plots were clipped during the last week of August 2005 and vascular plants collected and separated by species. Standing dead biomass was also collected, but dead biomass lying on the ground (litter) was discarded. With the exception of one plot with 50% sedge cover, the contribution of sedges to the total plot percent cover, and therefore to total leaf area, was minimal (Table 1). Due to the methodological difficulties in directly measuring sedge LAI, the contribution of sedges to total LAI was

neglected and the above plot with 50% sedge cover was not considered in the subsequent analysis.

The leaf area of each plot was calculated planimetrically. One randomly selected subsample of leaves was scanned (300 dpi) for each shrub species of each plot, using a standard desktop scanner (CanoScan LIDE 30, Canon USA Inc., Lake Success, New York, USA). Shrub species with flat leaves (*V. myrtilloides*, *K. angustifolia*, *C. calyculata*) were scanned pressed, and shadow around the leaf margins created by the scanning process was removed after posterizing the scan with the Corel Photo-Paint (v10) raster graphics software (Corel Corp., Ottawa, Ontario, Canada). Posterization converts a RGB image into a limited number of distinct colours that can be separately processed. For our purposes, posterizing the scans into four distinct colours allowed extraction of the shadow around the leaves. Species with non-flat leaves (*L. groenlandicum*, *K. polifolia*, *A. glaucophylla*) were first scanned “un-pressed” and then pressed, followed by shadow removal through posterization. Subsequently, leaf area for all scans was determined using the WinSeedle (v2003a) image analysis software (Regent Instruments Inc., Quebec City, Quebec, Canada). To comply with the definition of LAI by Chen and Black (1992) as one-half the total radiation intercepting leaf area per unit ground horizontal surface area, leaf area of shrub species with non-flat leaves was taken as the arithmetic mean of the leaf area obtained from “un-pressed” and the pressed scans.

Total leaf and woody material was weighted separately for each species. The “true” shrub LAI of each plot (L) was calculated as:

$$L = \sum \frac{W_{\text{tot}}}{A_{\text{plot}}} \left(\frac{A_{\text{ss}}}{W_{\text{ss}}} \right) \quad (1)$$

where W_{tot} is the total weight of leaves per species of each plot [g], A_{plot} the area of the plot [m²], A_{ss} the leaf area obtained for each species subsample [m²], and W_{ss} is the weight of leaves of each species subsample [g].

2.3. Indirect LAI measurements

Indirect measurements of shrub LAI were performed with the LAI-2000 plant canopy analyzer a few days prior to clipping in mid-August 2005. This optical sensor measures canopy gap fraction by detecting blue diffuse light between 400 and 490 nm penetrating the canopy at five concentric rings, corresponding to 0–13° (ring 1), 16–28° (ring 2), 32–43° (ring 3), 47–58° (ring 4), and 61–74° (ring 5) zenith angles. LAI-2000 measurements are ideally taken under diffuse sky conditions with no direct sunlight, i.e. at dusk or dawn or under overcast conditions. By utilizing the blue part of the electromagnetic spectrum for the measurement of canopy gap fraction, the effect of multiple light scattering within a canopy is minimized, albeit not entirely avoided because of the scattering albedo of leaves at blue wavelengths. The calculation of LAI_e from the LAI-2000 measurement is based on inversion of Beer's Law, assuming a random spatial distribution of light intercepting canopy elements:

$$P(\theta) = e^{-G(\theta)L_e/\cos\theta_e} \quad (2)$$

where $P(\theta)$ is the measured canopy gap fraction at the zenith angle θ and $G(\theta)$ the projection coefficient characterizing the angular distribution of light intercepting canopy elements at the zenith angle θ , and L_e is the LAI_e. The calculation of the L_e without prior knowledge of $G(\theta)$ requires the measurement of $P(\theta)$ over the hemisphere with Miller's (1967) theorem:

$$L_e = 2 \int_0^{\pi/2} \ln \left[\frac{1}{P(\theta)} \right] \cos\theta \sin\theta d\theta \quad (3)$$

The hemispherical measurement of $P(\theta)$ is considered to be adequately approximated by measuring $P(\theta)$ at the five discrete zenith angles 7°, 23°, 38°, 53°, and 68° (i.e. the mid-points of the five concentric rings), and the LAI_e obtained from the LAI-2000 instrument is simply the summation over the five mid-points.

LAI_e includes the contribution of all canopy elements (i.e. green and dead leaves, branches, tree trunks including attached moss and lichen) to light interception and does not account for foliage clumping effects that might occur at different spatial scales within a canopy. Based on theoretical considerations and subsequent validation, Chen (1996) and Chen et al. (1997) introduced the following equation to derive LAI (L) from LAI_e (L_e):

$$L = (1 - \alpha)L_e \frac{\gamma_E}{\Omega_E} \quad (4)$$

where α is the woody-to-total leaf area ratio (to account for the contribution of woody canopy elements to light interception through $(1 - \alpha)$), γ_E the needle-to-shoot area ratio (to account for foliage clumping within shoots), and Ω_E is the element clumping index (to account for foliage clumping at spatial scales larger than the average primary foliage element size, i.e. leaves for broadleaf species, and shoots for coniferous species). Whereas LAI_e can be measured easily and accurately with the LAI-2000 instrument, the reliable determination of γ_E , Ω_E , and α is a critical component in optical LAI measurements and especially α still remains a challenge (Chen et al., 2006).

Since the shrub layer of the Mer Bleue bog comprises six broad-leaf shrub species, five evergreen and one deciduous, individual leaves are considered as primary foliage elements, which makes a correction to Ω_E through γ_E not necessary, and, thus, $\gamma_E = 1$ (Chen et al., 1997). Unlike in forest canopies, where leaves are clumped around a central axis (whether twigs, branches, or trunks), we consider, based on visual inspection, the spatial distribution of all light intercepting elements of the shrub canopy at the Mer Bleue bog to be approximately random (Fig. 2). Therefore, no correction for foliage clumping was applied to Eq. (4), i.e. $\Omega_E = 0.1$. As a result of $\gamma_E = 1$ and $\Omega_E = 1$, Eq. (4) simplifies to:

$$L = (1 - \alpha)L_e \quad (5)$$

The largest source of uncertainty in (4) and (5) is considered to be α . Its reliable estimation ideally requires destructive sampling (Chen et al., 2006). The inventory of the plots revealed that the abundance of woody canopy elements due the architecture of the



Fig. 2. Example of one of the 33 plots of 0.5 m × 0.5 m used in this study. The species present in this evergreen hummock plot are *Chamaedaphne calyculata* (95% of total percent cover) and *Kalmia angustifolia* (5% of total percent cover).

shrub canopy (Fig. 2) might significantly affect the LAI-2000 measurements. Optical approaches to determine α such as the Multiband Vegetation Imager (MVI; Kucharik et al., 1998) or the approach pursued by Barr et al. (2004) based on non-growing and growing season LAI-2000 measurements were both not feasible due to the height and the architecture of the shrub canopy (for MVI) and the evergreen nature of five of the six major shrub species (for the LAI-2000 instrument-based approach), respectively. We destructively determined α for five of the six major shrub species of the Mer Bleue bog (*C. calyculata*, *L. groenlandicum*, *K. angustifolia*, *K. polifolia*, and *V. myrtilloides*). Since *A. glaucophylla* only minimally contributed to the total plot percent cover of just two plots (data not shown), α for this species was taken as the mean of α of the major five shrub species. For each shrub species measured, we took three subsamples of woody material from different plots, separated them into their basic elements (twigs, branches, and trunks), and calculated their total woody areas (A_{w-ss}) based on their morphological characteristics as truncated cones (conical frustum: a frustum created by slicing the top of a cone with the cut made parallel to the base), not including the top and the base circles with:

$$A_{w-ss} = \pi \left(\sum r_1 + \sum r_2 \right) \sqrt{\left(\sum r_1 - \sum r_2 \right)^2 + \sum h^2} \quad (6)$$

where r_1 and r_2 are the top and the base radii [m] of each basic woody element, and h the length [m] of each basic woody element. The woody area index (W_{species}) of each species per plot was calculated similar to Eq. (1) with:

$$W_{\text{species}} = \left[\frac{A_{w-ss} W_{\text{tot}}}{W_{ss}} \right] \frac{1}{A_{\text{plot}}} \quad (7)$$

where A_{w-ss} is the total woody area obtained for each subsample [m²] through Eq. (6), W_{tot} the total weight of woody material of the species per plot [g], W_{ss} the weight of woody material of each species subsample [g], and A_{plot} is the area of the plot [m²]. Finally, α was calculated for each species as the average of three subsamples using (Kucharik et al., 1998):

$$\alpha = \frac{W_{\text{species}}}{W_{\text{species}} + L_{\text{species}}} \quad (8)$$

where W_{species} is the woody area index of each species per plot calculated with Eq. (7), and L_{species} the leaf area index for each species per plot calculated as part of Eq. (1).

LAI-2000 measurements were taken under suboptimal sky conditions during the day with partial direct sunlight. Considering the small area of each plot we emulated ideal sky conditions by creating enough shadow to avoid direct illumination of the shrub canopy and its vicinity. Therefore, it can be assumed that the multiple light scattering within the shrub canopy due to direct illumination was kept to a minimum. Shadowing of the plots was accomplished by positioning the operator of the LAI-2000 instrument and an additional person between the plot and the instrument sensor, and the sun. To avoid any effects of the two people on the sensor of the LAI-2000 instrument, the 270° view cap provided by LI-COR was used for all measurements.

For each plot we measured diffuse radiation above the shrub canopy for reference, followed by five measurements below the shrub canopy, four taken between the four corners and the center, and one taken at the center of the LAI plot, followed by another reference measurement above the shrub canopy. The post-processing of the measurements was accomplished using the LAI-2000 analysis software provided by LI-COR (F2000.exe). For each of the five individual below-canopy measurements per plot, an interpolated above-canopy reference based on the “before” and “after” above-canopy reference measurement was used. LAI_e of each plot was calculated as the arithmetic mean of the five measurements below the shrub canopy.

A common way to investigate the effect of multiple scattering of blue light within a canopy on the LAI-2000 measurement is to ignore rings 4 and 5 in the post-processing of the LAI-2000 data with F2000.exe (Chen et al., 2006). Thereby, the largest zenith angles where the effect of multiple light scattering is usually the strongest are excluded from the LAI_e calculation, theoretically resulting in an increase of LAI_e compared to its calculation based on all five rings. The assumption underlying this simple approach is random angular distribution of light intercepting canopy elements (Chen et al., 2006), i.e. $G(\theta) = 0.5$ in Eq. (2). The validity of this assumption for the shrub canopy in the bog was tested for each ring by calculating $G(\theta)$ through inversion of Eq. (2) using $P(\theta)$ from the instrument raw data, and LAI_e of each ring calculated with F2000.exe. However, it has to be noted at this point that the interpretation of the impact of excluding rings 4 and 5 from the calculation of LAI_e is still of ongoing scientific dispute in the literature (Leblanc and Chen, 2001; Planchais and Pontailier, 1999). A recent summary of this dispute is provided by Hyer and Goetz (2004). For forest stands, Chen et al. (2006) maintain that multiple light scattering at rings 4 and 5

Table 2
Summary statistics of the “true” shrub LAI at Mer Bleue bog of 32 plots according to microform

Microform	#	Mean LAI [m ² /m ²]	Standard deviation [m ² /m ²]	Scheffe’s multiple comparisons
Hollow ^a	8	0.82	0.30	A
Evergreen hummock	9	1.92	0.40	B
Deciduous hummock	6	2.18	0.28	B
Lawn	9	1.21	0.53	A

For Scheffe’s multiple comparisons, the mean “true” shrub LAI of the microforms with the same letters are not significantly different.

^a One of the 33 plots with 50% sedge cover was excluded from the analysis.

induced multiple light scattering effects that decreased LAI_e by 16%.

For our objective to investigate the combined effect of microtopographic position of the LAI-2000 measurement location on LAI_e and multiple light scattering, we followed the same procedure as described above, i.e. excluding rings 4 and 5 from the calculation of LAI_e. In the following, LAI_e and LAI based on rings 1 through 5 are referred to as LAI_{e-12345} and LAI₁₂₃₄₅, respectively, and LAI_e and LAI based on rings 1, 2, and 3 are referred to as LAI_{e-123} and LAI₁₂₃, respectively.

2.4. Statistical analysis

We tested the differences of “true” shrub LAI between the four different microforms using an ANOVA followed by Scheffe’s test for post hoc multiple comparisons. Due to the non-normal distribution of the calculated projection coefficients, $G(\theta)$, as determined with the Shapiro–Wilk test, we applied the non-parametric Wilcoxon signed-rank test to test for a statistically significant difference of $G(\theta)$ from 0.5. We assessed the differences in LAI_e after exclusion of rings 4 and 5, i.e. the differences between LAI_{e-12345} and LAI_{e-123}, per microform using paired t -tests. The impact of using a general average value of α instead of a plot-specific average weighted according to percent cover was assessed using an F -test. Finally, the coefficient of determination (R^2), F -tests for the statistical significance of the differences of the slopes of the linear correlations from 1 and of the intercepts from 0, and the root mean square error (RMSE) between “true” shrub LAI and optically measured shrub LAI were used as statistical tools for the performance evaluation of the LAI-2000 instrument. Instead of commonly used R^2 or RMSE, the closeness of the linear correlation to the ideal 1:1-line, as quantified by the p -values for slope = 1 and intercept = 0, was our main criterion of evaluation. The level of significance of all statistical tests was fixed at 0.05 and statistical analyses were conducted with the SAS (v9.1) statistical analysis software (SAS Institute Inc., Cary, North Carolina, USA).

3. Results

3.1. General trends of shrub LAI at the Mer Bleue bog

“True” shrub LAI of the 32 plots ranged from 0.25 to 2.50 and varied spatially according to microform. Deciduous hummocks had the highest mean “true” shrub LAI (2.18), followed by evergreen hummocks (1.92), and lawns (1.21). Hollows were characterized by the lowest mean “true” shrub LAI (0.82). The effect of microform on “true” shrub LAI was significant (ANOVA, $p < 0.0001$), with hollows and lawns, and evergreen and deciduous hummocks groups significantly different from each other (Table 2).

3.2. Effect of the contribution of woody shrub canopy elements on the performance of the LAI-2000 instrument

The woody-to-total area ratios, α , for shrub species ranged from 0.23 to 0.32 (Table 3). These values are a critical component in the application of optical techniques for the indirect measurement of LAI using either Eq. (4) or Eq. (5). To our knowledge, to date there has been no study reporting species-specific estimates of α for shrub species characteristic for ombrotrophic peatlands. Comparison of Table 3 with published estimates of α for tree species ranging from 0.03 to 0.32 (Chen, 1996) shows that the contribution of woody

Table 3
Species-specific woody-to-total area ratios, α , for the five major shrub species of Mer Bleue bog determined through destructive sampling

Species	#	Mean, α	Standard deviation
<i>Chamaedaphne calyculata</i>	3	0.26	0.0382
<i>Ledum groenlandicum</i>	3	0.26	0.0196
<i>Kalmia angustifolia</i>	3	0.24	0.0261
<i>Kalmia polifolia</i>	3	0.32	0.0460
<i>Vaccinium myrtilloides</i>	3	0.23	0.0183
<i>Andromeda glaucophylla</i> ^a	–	0.26	–

^a Taken as the mean of α of the major five shrub species.

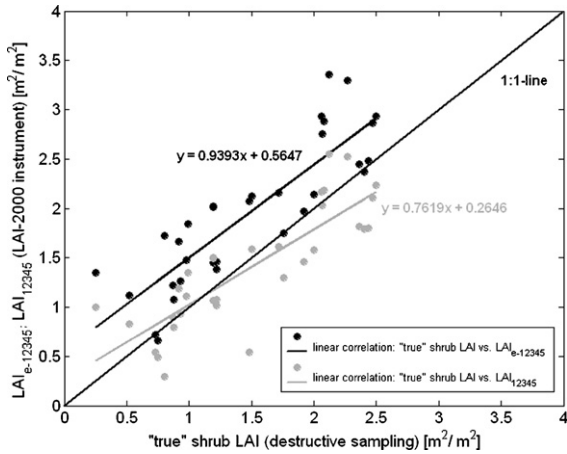


Fig. 3. Effect of correcting LAI_{e-12345} for the contribution of woody canopy elements to light interception through species-specific woody-to-total area ratios, α (Table 3), on the linear correlation between “true” shrub LAI and LAI₁₂₃₄₅.

canopy elements to light interception is quite considerable at the Mer Bleue bog.

LAI_{e-12345} was corrected for the contribution of woody canopy elements resulting in LAI₁₂₃₄₅ based on Eq. (5) using the species-specific estimates of α provided in Table 3, weighted according to percent cover of each species (data not shown). The linear correlation between “true” shrub LAI and LAI_{e-12345} and LAI₁₂₃₄₅, respectively, for the 32 plots is good (Fig. 3). R^2 and RMSE are 0.74 and 0.60, respectively, for LAI_{e-12345} and 0.69 and 0.38, respectively, for LAI₁₂₃₄₅, indicating the general applicability and usefulness of the LAI-2000 instrument to provide a quick and reliable shrub LAI estimate after correcting LAI_e for α . We also corrected LAI_{e-12345} for the contribution of woody canopy elements resulting in LAI₁₂₃₄₅ based on Eq. (5) using an average value of 0.26 of the species-specific estimates provided in Table 3. The linear correlations are not significantly different ($p = 0.9097$).

Table 4 summarizes the characteristics of the linear correlations of Fig. 3, statistically demonstrating the effects of correcting LAI_{e-12345} through α to obtain

LAI₁₂₃₄₅. R^2 of LAI₁₂₃₄₅ is slightly reduced after the correction through α compared to LAI_{e-12345}. The reduced RMSE of LAI₁₂₃₄₅ compared to LAI_{e-12345} indicates a decrease in error between “true” shrub LAI and indirectly measured LAI. The correction through α moves the intercept of the linear correlation closer to 0, but decreases its slope, which after the correction is significantly different from 1. However, it can be seen that for both, LAI_{e-12345} and LAI₁₂₃₄₅, the slopes are less than 1, meaning that the LAI-2000 instrument tends to generally underestimate “true” shrub LAI in the higher range, but to overestimate “true” shrub LAI in the lower range. These tendencies are related to microtopography and multiple light scattering, as will be demonstrated in the following section.

3.3. Combined effect of microtopography and multiple light scattering on the performance of the LAI-2000 instrument

To allow for the reliable investigation of the combined effect of the microtopographic position of the LAI-2000 measurement location and multiple light scattering based on the simple approach of excluding rings 4 and 5, it is mandatory for the underlying assumption of random angular distribution of light intercepting canopy elements of the multiple light scattering component to be generally valid (i.e. $G(\theta) \cong 0.5$). For each plot, projection coefficients, $G(\theta)$, were calculated through inversion of Eq. (2) based on the measured gap fraction, $P(\theta)$, and LAI_{e-12345}, separately derived from each ring of the LAI-2000 instrument. Application of the non-parametric Wilcoxon signed-rank test to the calculated projection coefficients summarized in Table 5 revealed that there are no statistically significant differences between $G(\theta) = 0.5$ and the calculated mean projection coefficients.

As a result, the angular distribution of light intercepting canopy elements of the Mer Bleue bog shrub canopy can be considered to be random and the differences between LAI_{e-12345} and LAI_{e-123} were interpreted as fully caused by the combined effect of microtopographic position of the LAI-2000 measurement location and multiple light scattering.

Table 4
Summarized characteristics of the linear correlations of Figs. 3 and 6

Linear correlation	Intercept	Slope	R^2	p (model)	p (intercept = 0)	p (slope = 1)	RMSE
“True” shrub LAI vs. LAI _{e-12345}	0.56	0.94	0.74	<0.0001	0.0020	0.5582	0.5990
“True” shrub LAI vs. LAI ₁₂₃₄₅	0.26	0.76	0.69	<0.0001	0.0926	0.0163	0.3775
“True” shrub LAI vs. LAI _{e-123}	0.23	1.28	0.75	<0.0001	0.2944	0.0419	0.8325
“True” shrub LAI vs. LAI ₁₂₃	0.16	0.97	0.74	<0.0001	0.3575	0.7489	0.3846

Table 5

Projection coefficients, $G(\theta)$, calculated from measured gap fraction, $P(\theta)$, for each plot and $LAI_{e-12345}$ for each ring of the LAI-2000 instrument

Ring	#	Min. $G(\theta)$	Max. $G(\theta)$	Mean $G(\theta)$	Standard deviation	p (Wilcoxon)
1	32	0.3383	0.8092	0.4869	0.0787	0.2403
2	32	0.4126	0.6621	0.4963	0.0467	0.4757
3	32	0.4195	0.5779	0.4983	0.0292	0.5185
4	32	0.4496	0.5466	0.4996	0.0163	0.3592
5	32	0.4626	0.5165	0.4986	0.0078	0.1778

Exclusion of rings 4 and 5 in the post-processing of the LAI-2000 instrument raw data modified LAI_e in a consistent manner for most microforms. Contrasting lawns, the differences between $LAI_{e-12345}$ and LAI_{e-123} for hollows, evergreen, and deciduous hummocks are statistically significant. In hollows, exclusion of rings 4 and 5 resulted in a mean decrease in LAI_e of around 6% (Fig. 4). Not included in this calculation was one further hollow plot that shows a 12% increase in LAI_e after exclusion of rings 4 and 5. On both, evergreen and deciduous hummocks, exclusion of rings 4 and 5 resulted in a mean increase in LAI_e of around 10% and 22%, respectively. Contrary to hollows, and evergreen and deciduous hummocks, there is no clear trend in LAI_e change on lawns. For this microform, exclusion of rings 4 and 5 did not affect LAI_e on average since for five plots, LAI_e shows a mean 6% increase and for four plots LAI_e shows a mean 7% decrease. As revealed by our plot inventory, the former five plots were located on approximately horizontal lawn portions, whereas the latter four plots were located on slightly lowered lawn portions, showing a mean decrease in LAI_e similar to hollows. Thus, we fully attributed the

observed mean 6% increase in LAI_e of the former five plots to multiple light scattering, since the LAI-2000 measurements of these plots were not influenced by their microtopographic positions. However, the net change in LAI_e for lawn plots was considered to be negligible.

Hummocks represent the highest microtopographic positions of the Mer Bleue bog surface (Fig. 5). The pathlength through a plant canopy increases with zenith angle. Therefore, the canopy gap fraction measured by the LAI-2000 instrument is lowest at the largest zenith angle. Due to the lower elevation of the shrub canopy in the vicinity of hummocks the pathlengths through the shrub canopy at large zenith angles are smaller than the case when the shrub canopy is horizontal. Thus, in addition to the underestimation of LAI_e due to multiple light scattering, LAI_e is further underestimated on hummocks due to these reduced pathlengths when all five rings are used in the post-processing of the LAI-2000 measurement. As a result, the observed mean 16% increase in LAI_e for both evergreen and deciduous hummocks shown in Fig. 4 can be attributed to the combined effect of microtopographic position of the LAI-2000 measurement location and to multiple light scattering. Based on the above observation of a mean 6% increase in LAI_e on horizontal lawn plots, the contribution of microtopography to the combined effect of microtopography and multiple light scattering on LAI_e was estimated as $16\% - 6\% = 10\%$ on average.

Hollows represent the lowest microtopographic position of the Mer Bleue bog surface (Fig. 5). Contrasting hummocks, in hollows the general increase of LAI_e due to multiple light scattering was counterbalanced by the microtopographic position of the LAI-2000 measurement location. That is, vegetation on the sides delineating hollows and the sides themselves reduced or even prevented the probabilities of diffuse light penetration at large zenith angles, causing considerable increase in LAI_e when all five rings were used in the post-processing. Exclusion of rings 4 and 5 resulted in a mean decrease of LAI_e since this view blockage was “removed” from the instrument sensor’s

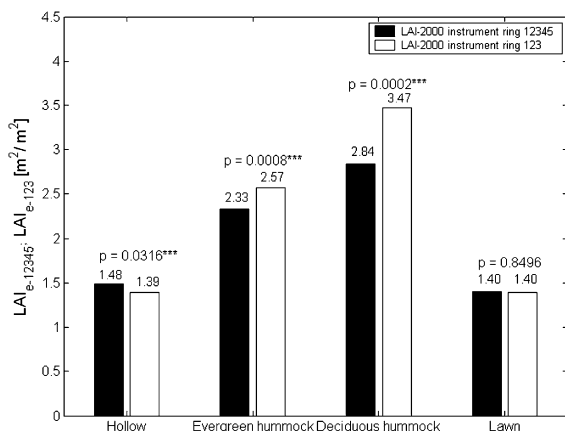


Fig. 4. Mean effects of excluding rings 4 and 5 in the post-processing of the LAI-2000 instrument raw data ($LAI_{e-12345}$), resulting in LAI_{e-123} , per microform (no errorbars are presented since the analysis is based on a paired t -test, for which errorbars would be misleading).

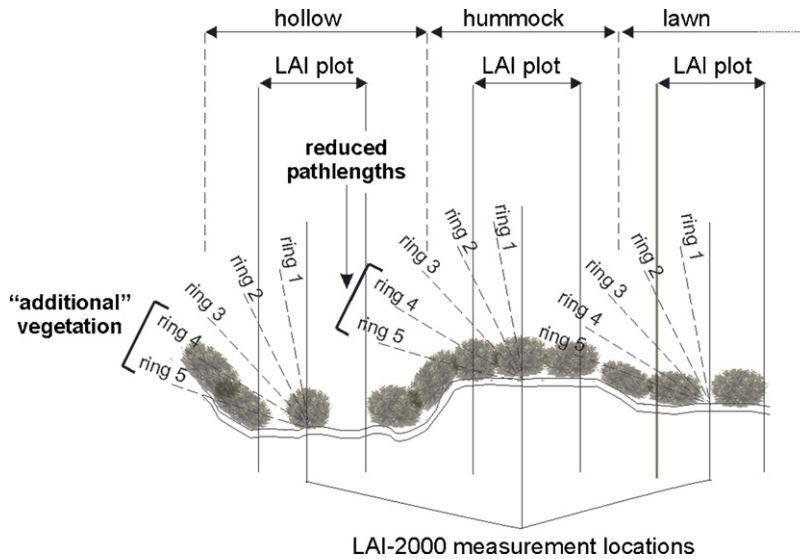


Fig. 5. Effect of microtopography on the LAI-2000 measurement (not drawn to scale).

field of view. The clear increase in LAI_e for one hollow plot was most likely caused by the fact that this plot was not clearly distinct from its immediate vicinity in terms of relief, and, thus, exclusion of rings 4 and 5 simply resulted in the combined effect of microtopography and multiple light scattering as observed on hummocks. For hollow and slightly lowered lawn plots, the contribution of microtopography to the combined effect of microtopography and multiple light scattering on LAI_e was estimated as $(-6\%) - 6\% = -12\%$ on average, assuming that the contribution of multiple light scattering to the combined effect is also 6% on average.

3.4. Overall performance of the LAI-2000 instrument

Fig. 6 shows the linear correlations between “true” shrub LAI and LAI_{e-123}, and between “true” shrub LAI and LAI₁₂₃, respectively, for the 32 plots. The overall effect of excluding rings 4 and 5 and correcting for the woody canopy elements through α on the characteristics of the linear correlations shown in Fig. 6 are provided with Table 4. As expected, the linear correlations are good, with $R^2 = 0.75$ and RMSE = 0.83 for LAI_{e-123}, and $R^2 = 0.74$ and RMSE = 0.38 for LAI₁₂₃, respectively, and, thus, are in the same range as for LAI_{e-12345} and LAI₁₂₃₄₅. However, for the objectives of our contribution, these two statistical measures are not fully adequate to demonstrate the overall positive effect of excluding rings 4 and 5 and correcting for the woody canopy elements through α on the linear correlation of Fig. 6. Once both factors are considered, both intercept and slope of the linear correlation between “true” shrub LAI and LAI₁₂₃ are not significantly different from 0 and 1, respectively. Under the assumptions that the combined effect of microtopography and multiple scattering is more or less entirely removed through excluding rings 4 and 5, and that the contribution of woody canopy elements to light interception is accounted for correctly through α , these results indicate that Ω_E for the shrub canopy has to be close to unity, i.e. $\Omega_E \cong 1$.

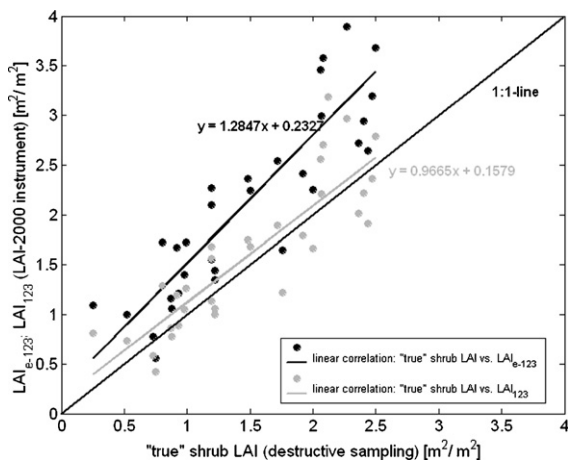


Fig. 6. Overall effect of excluding rings 4 and 5 (i.e., LAI_{e-123}) and correcting for the woody canopy elements to light interception through species-specific woody-to-total area ratios, α (Table 3), on the linear correlation between “true” shrub LAI and LAI₁₂₃.

The spatial variability of “true” shrub LAI according to microform as outlined in 3.1 is captured for the most part by LAI₁₂₃, with the difference that lawns are

Table 6

Summary statistics of LAI₁₂₃ at the Mer Bleue bog of 32 plots according to microform

Microform	#	Mean LAI [m ² /m ²]	Standard deviation [m ² /m ²]	Scheffe's multiple comparisons
Hollow ^a	8	1.11	0.3119	A
Evergreen hummock	9	1.90	0.4221	B
Deciduous hummock	6	2.62	0.4848	C
Lawn	9	1.05	0.4826	A

For Scheffe's multiple comparisons, the mean "true" shrub LAI of the microforms with the same letters are not significantly different.

^a One of the 33 plots with 50% sedge cover was excluded from the analysis.

characterized by the lowest mean LAI₁₂₃ and not hollows (Table 6). Similar to "true" shrub LAI, the effect of microform on LAI₁₂₃ is significant (ANOVA, $p < 0.0001$), with LAI₁₂₃ for the different microforms significantly different from each other, with the exception of hollows and lawns.

A possible explanation for the slight differences between "true" shrub LAI and LAI₁₂₃ as outlined in Tables 2 and 6, respectively, is provided in Fig. 7, presenting the linear correlation between "true" shrub LAI and LAI₁₂₃ of Fig. 6 with respect to the microtopographic position of the individual plots. Generally, shrub LAI obtained from the LAI-2000 instrument for hollow and deciduous hummock plots was overestimated, whereas for evergreen hummock and lawn plots it was underestimated. These tendencies to over- and underestimate shrub LAI dependent on microform are most likely related to the different nature and architecture of the species prevalent in different microforms as influenced by different heights of the peatland surface above the water table (Fig. 1). Contrasting lawns, and evergreen and deciduous hummocks, we assume that in hollows, LAI₁₂₃ based on the LAI-2000 measurement was overestimated. Besides having the lowest mean "true" shrub LAI, the shrub canopy in this microform is very sparse, and, thus,

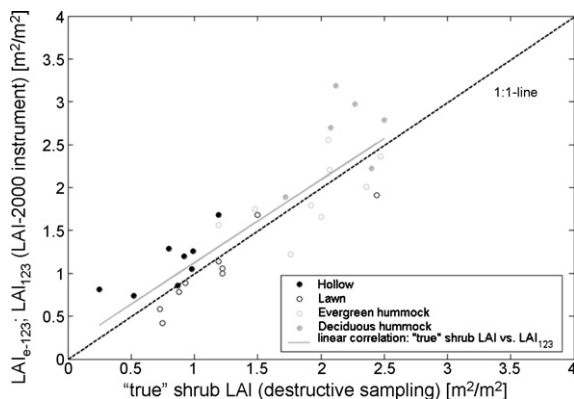


Fig. 7. Linear correlation of "true" shrub LAI and LAI₁₂₃ with respect to microtopographic position of the individual plots.

the assumption used in this study of no foliage clumping effects (i.e., $\Omega_E = 1$ in Eq. (5)) might not be fully valid anymore.

Another possible source for the observed over- and underestimation in Figs. 6 and 7 might be related to our methodology of shadow removal using posterization as part of the calculation of "true" shrub LAI. Lawns and evergreen hummocks, both overestimated by "true" shrub LAI, are dominated by *C. calyculata*, whereas deciduous hummocks, underestimated by "true" shrub LAI, are dominated by *V. myrtilloides*. *C. calyculata* are generally characterized by relatively thick leaves compared to *V. myrtilloides*. As a result, more shadow was produced by *C. calyculata* leaves than by *V. myrtilloides* leaves during the scanning process. It cannot be guaranteed that with the pursued approach of using posterization for shadow removal, the correct amount of shadow was captured for both species, probably resulting in underestimation "true" shrub LAI for deciduous hummocks dominated by *V. myrtilloides* and overestimation of "true" shrub LAI for hollow and evergreen hummocks dominated by *C. calyculata*.

4. Conclusion

Two linked characteristic features of ombrotrophic peatlands that play a fundamental role in their overall functioning are microtopography and a more or less continuous shrub canopy. The LAI of the shrub canopy is studied by adapting an established equation developed for boreal forest canopies by Chen (1996) and Chen et al. (1997). Key parameters in the equation are evaluated for applications to shrubs underlain by pronounced microtopography in an ombrotrophic peatland using direct and indirect LAI measurement techniques. Based on this research, we suggest the following practice for the application of the LAI-2000 instrument to shrub canopies of ombrotrophic peatlands (in order of importance):

- (I) to exclude rings 4 and 5 from the post-processing of the LAI-2000 instrument raw data as a means to

- eliminate the combined effect of the microtopographic position of the LAI-2000 measurement location and multiple light scattering;
- (II) to account for the contribution of woody canopy elements to light interception by using species-specific woody-to-total area ratios as provided in Table 3 (or, in case of shrub species composition and percent cover similar to the Mer Bleue bog, an average woody-to-total area ratio of 0.26);
- (III) to calculate shrub LAI from LAI_c using Eq. (5) under the assumption of no foliage clumping effects.

Acknowledgements

This work was supported by the Fluxnet Canada Research Network funded by the Natural Science and Engineering Research Council of Canada, the Canadian Foundation for Climate and Atmospheric Sciences and BIOCAP Canada. We gratefully acknowledge the help of Philippe Samson-Toussaint, Nick Phelps, David Brodkey, and Sam Price in the field. We thank Dr. Ian Strachan from McGill University for providing us with the LAI-2000 instrument and Ajit Govind from the University of Toronto for the fruitful discussions during the preparation of this manuscript. Dr. Tim Moore from McGill University is thanked for insightful comments and suggestions that improved the quality of this manuscript. We also thank the two anonymous reviewers for their careful reading and helpful comments on an earlier draft of this manuscript.

References

- Barr, A.G., Black, T.A., Hogg, E.H., Kljun, N., Morgenstern, K., Nesic, Z., 2004. Inter-annual variability of leaf area index of boreal aspen-hazelnut forest in relation to net ecosystem production. *Agr. Forest Meteorol.* 126, 237–255.
- Bréda, N.J.J., 2003. Ground-based measurements of leaf area index: a review of methods, instruments and current controversies. *J. Exp. Bot.* 54, 2403–2417.
- Bubier, J.L., Moore, T.R., Crosby, G., 2006. Fine-scale vegetation distribution in a cool temperature peatland. *Can. J. Bot.* 84, 910–923.
- Chen, J.M., Black, T.A., 1992. Defining leaf area index for non-flat leaves. *Plant Cell Environ.* 15, 421–429.
- Chen, J.M., 1996. Optically-based methods for measuring seasonal variation of leaf area index in boreal conifer stands. *Agr. Forest Meteorol.* 80, 153–163.
- Chen, J.M., Rich, P.M., Gower, S.T., Norman, J.M., Plummer, S., 1997. Leaf area index of boreal forests: theory, techniques, and measurements. *J. Geophys. Res.* 102, 29429–29443.
- Chen, J.M., Govind, A., Sonnentag, O., Zhang, Y., Barr, A., Amiro, B., 2006. Leaf area index measurements at Fluxnet Canada forest sites. *Agr. Forest Meteorol.* 140, 257–268.
- Clymo, R.S., 1998. Carbon accumulation in peatland. *Oikos* 81, 368–388.
- Frolking, S., Roulet, N.T., Moore, T.R., Lafleur, P.M., Bubier, J.L., Crill, P.M., 2002. Modeling seasonal to annual carbon balance of Mer Bleue bog, Ontario, Canada. *Global Biogeochem. Cy.* 16, 1030 doi:10.1029/2001GB001457.
- Gorham, E., 1991. Northern peatlands: role in the carbon-cycle and probable responses to climatic warming. *Ecol. Appl.* 1, 182–195.
- Hyer, E.J., Goetz, S.J., 2004. Comparison and sensitivity analysis of instruments and radiometric methods for LAI estimation: assessments from a boreal forest site. *Agr. Forest Meteorol.* 122, 157–174.
- Jonckheere, I., Fleck, S., Nackaerts, K., Muys, B., Coppin, P., Weiss, M., Baret, F., 2004. Review of methods for in situ leaf area index determination—Part I. Theories, sensors and hemispherical photography. *Agr. Forest Meteorol.* 121, 19–35.
- Kucharik, C.J., Norman, J.M., Gower, S.T., 1998. Measurements of branch area and adjusting leaf area index indirect measurements. *Agr. Forest Meteorol.* 91, 69–88.
- Küßner, R., Mosandl, M., 2000. Comparison between direct and indirect estimation of leaf area index in mature Norway spruce stands of eastern Germany. *Can. J. Forest Res.* 30, 440–447.
- Lafleur, P.M., Roulet, N.T., Admiral, S.W., 2001. Annual cycle of CO₂ exchange at a bog peatland. *J. Geophys. Res.* 106, 3071–3081.
- Lafleur, P.M., Hember, R.A., Admiral, S.W., Roulet, N.T., 2005. Annual and seasonal variability in evapotranspiration and water table at a shrub-covered bog in southern Ontario, Canada. *Hydrol. Process.* 19, 3533–3550.
- Leblanc, S.G., Chen, J.M., 2001. A practical scheme for correcting multiple scattering effects on optical LAI measurements. *Agr. Forest Meteorol.* 110, 125–139.
- Liu, J., Chen, J.M., Cihlar, J., Park, W.M., 1997. A process-based boreal ecosystem productivity simulator using remote sensing inputs. *Remote Sens. Environ.* 62, 158–175.
- Maltby, E., Immirzi, P., 1993. Carbon dynamics in peatlands and other wetland soils regional and global perspectives. *Chemosphere* 27, 999–1023.
- Miller, J.B., 1967. A formula for average foliage density. *Aust. J. Bot.* 15, 144–151.
- Moore, T.R., Roulet, N.T., Waddington, J.M., 1998. Uncertainty in predicting the effect of climatic change on the carbon cycling of Canadian peatlands. *Clim. Change* 40, 229–245.
- Moore, T.R., Bubier, J.L., Frolking, S.E., Lafleur, P.M., Roulet, N.T., 2002. Plant biomass and production and CO₂ exchange in an ombrotrophic bog. *J. Ecol.* 90, 25–36.
- Norman, J., Welles, J., 1991. Instruments for indirect measurements of canopy architecture. *Agron. J.* 82, 818–825.
- Payette, S., Rochefort, L., 2001. *Écologie des tourbières du Québec-Labrador*. Les Presses de l'Université Laval, Sainte-Foy, Canada.
- Planchais, I., Pontailler, J.-Y., 1999. Validity of leaf areas and angles estimated in a beech forest from analysis of gap frequencies, using hemispherical photographs and a plant canopy analyzer. *Ann. For. Sci.* 56, 1–10.
- Roulet, N.T., Lafleur, P., Richard, P.J.H., Moore, T.R., Humphreys, E., Bubier, J., 2006. Contemporary carbon balance and late Holocene carbon accumulation in a northern peatland. *Glob. Change Biol.* 12, 1–15 doi:10.1111/j.1365-2486.2006.01292.x.
- Sonnentag, O., Chen, J.M., Roberts, D., Talbot, J., Halligan, K.Q., Govind, A. Mapping tree and shrub leaf area indices in an ombrotrophic peatland through multiple endmember spectral unmixing. *Remote Sens. Environ.*, in press.

- Tarnocai, C., Kettles, I.M., Lacelle, B., 2000. Peatlands of Canada Map. Geological Survey of Canada, Open File 3834. Scale 1: 6 500 000. Natural Resources Canada, Ottawa.
- Turunen, J., Tomppo, E., Tolonen, K., Reinikainen, A., 2002. Estimating carbon accumulation rates of undrained mires in Finland—application to boreal and subarctic regions. *Holocene* 12, 69–80.
- Wheeler, B.D., Proctor, M.C.F., 2000. Ecological gradients, subdivisions and terminology of north-west European mires. *J. Ecol.* 88, 187–203.